



Research paper

A finite element and finite difference mixed approach for modeling fault rupture and ground motion

Chunfang Meng^{*}, Hua Wang^{**}

Earth Resources Laboratory, Massachusetts Institute of Technology, Cambridge, MA, USA

ARTICLE INFO

Keywords:

Induced earthquake
Finite element
Finite difference
Fault rupture
Ground motion

ABSTRACT

We combine a finite element (FE) code, Defmod, and a finite difference (FD) code, OpenSWPC, in modeling fault rupture and resulting ground motion. The rupturing process is modeled by the FE code, while the ground motion is modeled by the FD code. The FE-FD binding follows two steps: First, evaluate the FD grid points motion when executing the FE code; and then, impose those moving grid points to the FD domain to drive wave propagation. In order to avoid performance bottleneck, we implement this FE-FD binding in parallel. To verify this mixed approach, we evaluate two SCEC benchmark problems. The resulting synthetic waveforms agree well with the other benchmark participants. The waveform comparisons suggest that the FE-FD mixed model has less attenuation than the pure FE model.

1. Introduction

Rigorously modeling earthquake induced by human activities or natural causes is desired. Azle earthquake swarm is associated with wastewater disposal, (Hornbach et al., 2015). Groningen earthquake swarm is associated with natural gas production, (Wees et al., 2014). Mt. Hood earthquake is associated with seasonal ground water recharge, (Saar and Manga, 2003). Soutz-sous-Forets earthquake is purposely triggered by a water injection experiment, (Baisch et al., 2010).

Fig. 1 illustrates the mechanism of earthquakes induced by reservoir depletion.

The pore pressure changes, due to depletion, cause reservoir compaction, and promote fault slip, marked by the green arrows. When the superposition of the induced shear stress and background shear stress, in blue, exceeds a critical level, the fault may undergo dynamic rupture, producing seismic radiation. The same causality also applies to injection induced seismicity, although the event locations would be different. A sophisticated numerical model that helps us to understand the correlation between fluid injection/production and seismic risks must cover the loading process as well as the fault rupture and seismic radiation process.

Fig. 2 demonstrates the work flow that correlates the fluid production or injection with the induced seismicity.

Jha and Juanes (2014) investigate the stress perturbation during the

injection using a quasi-static model. Baisch et al. (2010) assume a constant shear stress drop within a slipping fault patch. And, the stress drop, by a constant rate 90%, is transferred as stress increases from the slipping patch to its neighboring patches. In both studies, static friction criterion is used to determine when and where the fault slip shall start and stop without considering fault dynamics.

Carcione et al. (2015) assume an analytical relation between the pore pressure the seismic sources. For the given domain pressure evolution, seismic sources and radiation are generated by a dynamic model. The pressure and seismic source relation is for micro seismicity instead of damaging earthquake. To correlate the pore pressure change with the seismic risks, one needs to consider the poroelastic stress perturbation on the fault plane.

Another type of modeling work, e.g. SCEC benchmark (Harris et al., 2010), is focused on dynamic fault rupture and wave propagation. The numerical methods can be roughly grouped by variations of finite element and finite difference methods. The finite element group includes linear element method, e.g. Pylith by Aagaard et al. (2015), and higher order methods, e.g. spectral element implemented by Komatitsch and Tromp (2002) and Discontinuous Galerkin implemented by Breuer et al. (2014). The finite difference group mainly use staggered grid and traction at split node method, (Dalguer and Day, 2007).

The finite element (FE) code Defmod, (Ali, 2014), with its implicit-explicit hybrid solver, (Meng, 2017), has been demonstrated

^{*} Corresponding author.

^{**} Corresponding author.

E-mail addresses: cmeng@mit.edu (C. Meng), wanghua@mit.edu (H. Wang).

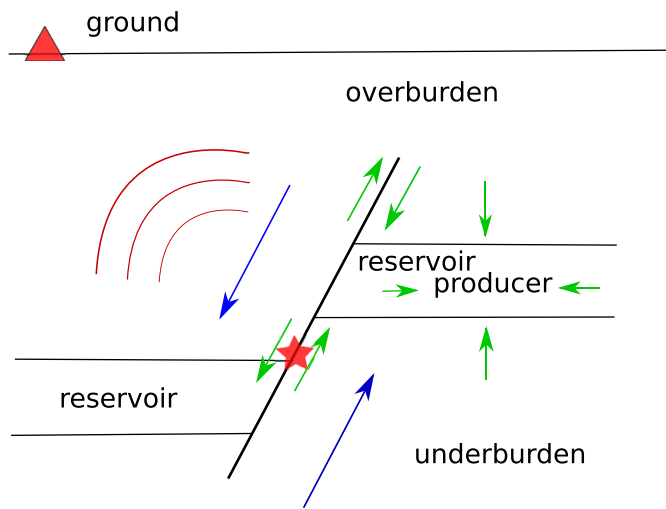


Fig. 1. Schematics of reservoir depletion induced earthquake.

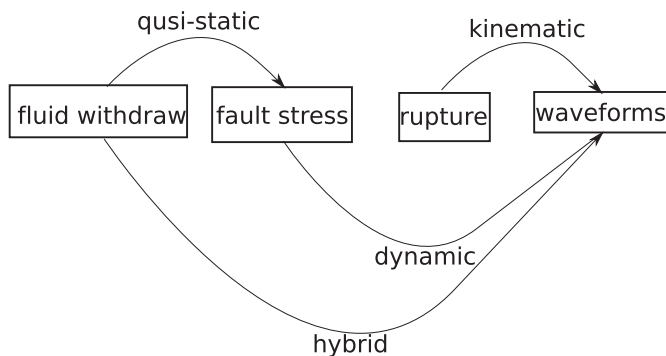


Fig. 2. Models connecting fluid production and seismic motions.

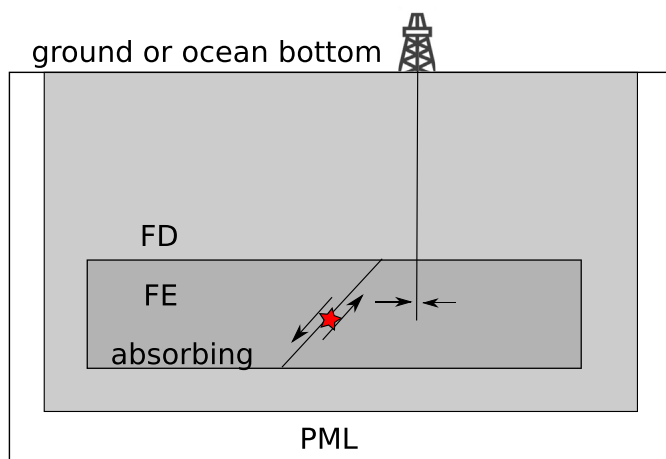


Fig. 3. Schematics for modeling reservoir depletion induced earthquakes.

capable of modeling both the inducing and dynamic rupture processes. The FE model, when running in parallel however, suffers the inter-computer communication cost. Also, the near-surface regions with low velocity pose a challenge to the explicit FE model. To obtain the desired waveform upper frequency, and for the explicit FEM model to meet the Courant-Friedrichs-Lewy (CFL) condition, both the element size and time step have to be small enough, which makes the model

computationally expensive. Improving the ground motion model performance has motivated this study. In Section 3, we compare different matrix-free methods, and explain why we choose to combine the FE code with a matrix-free finite difference (FD) code OpenSWPC, (Maeda et al., 2017). In this approach we make the FD domain adequately cover the near fault areas, and evaluate its near fault grid point motions when executing the FE code. The resulting grid point movements are then fed to the FD model as seismic sources for ground motion modeling.

With such combination, one could use FE method to model reservoir depletion, compaction and fault rupture, and use FD method to model ground motion at larger scale, which is illustrated by Fig. 3.

The FE domain is surrounded by viscous boundary, and the bottom and vertical sides of the FD domain are surrounded by perfectly matching layers (PML) to absorb the outgoing waves. The top of the FD domain can be free surface or ocean bottom.

2. A hybrid FE code Defmod

Ali (2014) gives a general introduction of the code. Meng (2017) provides detailed governing equation derivation from the differential (strong) forms to integration (weak) forms, see Appendix A. The FE code is capable of solving both the quasi-static problem for poro-(visco)-elastic processes, and dynamic problem for fault rupture and wave propagation. The code has gone through extensive verification against established analytical and numerical results, (Meng, 2017).

2.1. Quasi-static and dynamic problems

The quasi-static weak forms are based on (Smith and Griffiths, 2004). A pore fluid pressure stabilization method, (Bochev and Dohrmann, 2006), is applied. The Maxwell viscoelastic power law formulation is provided by Melosh and Raefsky (1980).

The dynamic weak form is based on (Zienkiewicz, 2000). The explicit solver employs Newmark time scheme and mass matrix lumping method. The frequency and time step limits are given by the Courant-Friedrichs-Lewy (CFL) criterion:

$$\Delta t \leq L / \sqrt{E/\rho},$$

$$f \leq 0.1 \sqrt{\mu/\rho} / L, \tag{1}$$

where L is the representative length of the elements, E and μ are the elastic moduli. Note that, $\sqrt{\mu/\rho}$ gives the shear wave velocity, which means one wavelength should be described by at least ten elements. From the desired upper frequency, density and elastic moduli, one can estimate the appropriate L and Δt . The problem size is determined by the domain scale and L .

A fault is modeled by split nodes, node pairs that coincide at the fault interface, but belong to different elements on different sides of the fault, see Appendix A. The split nodes motions are imposed by constraint equations to honor fault constitutive laws, e.g. slip weakening and rate-and-state friction. The implicit solver solves the weak form together with the constraint equations. The explicit solver employs the forward Lagrange multiplier method, Carpenter et al. (1991), to solve the weak form and constraint equations consecutively.

The resulting Lagrange multipliers approximate the traction required to keep the split nodes in stress balance. We limit the Lagrange multipliers, such that the fault would rupture when failure criterion is met (Bartolomeo et al., 2010) and Eq. (B.5).

2.2. Implicit-explicit solver hybridization (FE)

Fig. 4 demonstrates the structure of the hybrid solver.

The parent loop runs a quasi-static solver, and the child loop runs a dynamic solver. For every quasi-static step, the model examines the fault state against failure criterion to determine if a dynamic run shall be

Download English Version:

<https://daneshyari.com/en/article/6922175>

Download Persian Version:

<https://daneshyari.com/article/6922175>

[Daneshyari.com](https://daneshyari.com)